AFOSR TN 59-272
ASTIA AD 212 706

THE UNIVERSITY OF MICHIGAN

COLLEGE OF ENGINEERING
Department of Electrical Engineering
Solid State Devices Laboratories

Technical Report No. 8

MAGNETIC PROPERTIES OF POLYCRYSTALLINE MATERIALS

D.M. Grimes
R.D. Harrington
A.L. Rasmussen

UMRI-Project 2495

under contract with:

AIR FORCE OFFICE OF SCIENTIFIC RESEARCH
AIR RESEARCH AND DEVELOPMENT COMMAND
SOLID STATE SCIENCE DIVISION
CONTRACT NO. AF 18(603)-8

administered by:

THE UNIVERSITY OF MICHIGAN RESEARCH INSTITUTE ANN ARBOR

February, 1959

FOREWORD

Messrs. R.D. Harrington and A.L. Rasmussen are with the High Frequency Impedance Standards Section of the National Bureau of Standards, Boulder, Colorado. The spectral data were taken by them.

ABSTRACT

The variation of the magnetic Q with internal magnetization is discussed using both the domain rotation and the domain-wall motion model of magnetization change. The variation of the reversible susceptibilities with magnetic moment is reported on four samples, and the results are compared with results from the frequency spectra in the initial and remanent states. The distribution of magnetic moments in the system as a function of angle between individual and averaged moments is discussed in terms of an infinite series expansion in Legendre polynomials. The coefficients of the first four terms can be measured. Experimental data are given for the first three.

INTRODUCTION

The magnetic susceptibility is defined to be the ratio of resultant magnetization to magnetic field intensity. In ferrimagnets it is a function of both field strength and frequency. The reversible susceptibility is that susceptibility effective with a differential magnetic field. The differential field can be superimposed upon a finite biasing field. The reversible susceptibility depends upon the angle between biasing and differential fields, upon the magnetization level in the material, and upon the magnetic history of the specimen.

The susceptibility-producing mechanism is not completely understood. It is often assumed that either domain moments rotate in unison or that the domain walls move to change the net averaged moment of the sample. The reversible susceptibility and resulting differential magnetostriction for each mechanism were discussed and contrasted in an earlier paper, which will be referred to as I.[1]

In that paper, the reversible quantities were discussed in terms of the distribution of magnetic moments. The calculations of predicted behavior of the reversible quantities with magnetic moment were carried out with the assumption that the moments would be distributed in some most probable state determined by a Boltzman type distribution of moments about the unit sphere. This argument has the merit that the direction of the moments are strongly influenced by the crystallographic orientation, and that the orientation of neighboring grains can be considered to be independent. This does not mean, however, that the resulting moments must be randomly

oriented. A factor of considerable interest, therefore, is a calculation of what the distribution of moments is in a magnetic material.

The detailed calculation of $f(\theta)$ is possible, at this time, in only the simplest cases. The basic difficulty is that the solution of this problem must involve the solution of essentially the same number of coupled differential equations as there are atomic moments. If the moments are treated in the aggregate, localized potential minima between neighboring grains and neighboring domains must be included, as must the effect of nonmagnetic inclusions. The dominant role played by this type of surface energy has been stressed by Goodenough.[2]

The calculation of $f(\theta)$, then, requires first the development of as realistic as possible a microscopic model of magnetic behavior followed with the distribution of this behavior over the sample. The microscopic models used in I were (A) that the domain moments remained always oriented along the crystallographic directions which minimized the anisotropy energy, and (B) that the static moments remained along "easy" directions, but the susceptibility arose by the rotation of the domain moments away from those directions in the dynamic case. Neither model is completely correct. Both are highly idealized and, for example, contain neither the "curling" concept discussed by Brown[3] and by Frei, Shtrikman and Treves,[4] nor the effect of inhomogeneous fields. A more correct formulation awaits the inclusion of more accurate microscopic models.

There has, however, been ample precendent set for considering magnetic susceptibility as due to either domain rotation or to domain wall motion. This lamentable state is continued in this paper.

It was assumed in I that the frequency of the measuring field was much less than the resonance or relaxation frequency of the magnet. Under these conditions, the magnetization dependence of the transverse susceptibility on the biasing field is distinctly different for each of the assumed susceptibility sources as long as the anisotropy field remains much larger than the applied field.

The reversible susceptibility, as defined above, is reversible in the thermodynamic sense of zero energy dissipation for only the special case of zero applied frequency. An associated energy loss exists for all nonzero frequencies. This loss is describable as the imaginary part of the complex magnetic susceptibility, ($\chi = \chi' - j\chi''$). The magnetic Q is defined to be the ratio of real to imaginary susceptibility. It is convenient in the following section to discuss the loss in terms of Q. Q dependence upon magnetization, field directions, and source of susceptibility is briefly discussed in this paper.

Frequency spectra have commonly been used to investigate the susceptibility sources. This extensively used method depends upon the different dependence of the frequency of susceptibility fall-off on magnetization mechanism to distinguish between sources.[5,6,7,8] Some investigators have also measured the spectra of the material magnetized to remanence and have utilized these results to aid spectral interpretation.[9,10,11] Epstein[12] and Birks[13] in particular have utilized spectral information to obtain quantitative determinations of the amount of wall-motional and domain-rotational susceptibility.

DISCUSSION

Distribution Function $f(\theta)$

The macroscopic material is considered composed of randomly oriented crystallites. The crystallites are sufficiently small so that the moment of each crystallite is much less than the aggregate moment of the sample. The crystalline orientation of each grain is taken to be independent of the orientation of its neighbors. For such a model the static moment is always parallel with the static field.

The distribution $f(\theta) \sin \theta \, d\theta$ is defined to be the fraction of the atomic moments in the system oriented at an angle between θ and $\theta + d\theta$ with respect to the applied magnetic field. It is convenient to expand $f(\theta)$ in an infinite series of Legendre functions such that:

$$f(\theta) = \sum_{n=o}^{\infty} A_n P_n (\cos \theta) \tag{1}$$

where A_n is a function of the magnetic field present and the magnetic history of the specimen.

By definition,

$$\langle \cos^n \theta \rangle = \frac{\int d\Omega \cos^n \theta \, f(\theta)}{\int d\Omega f(\theta)} \tag{2}$$

where $\langle \cos^n \theta \rangle$ represents the average value of $\langle \cos^n \theta \rangle$ over the sample. Substituting Equation 1 into Equation 2 and integrating over the unit sphere yields:

$$\langle \cos^n \theta \rangle = \frac{1}{2A_o} \sum_{m=o}^{\infty} A_m \int_{-1}^{1} \gamma^n d\gamma P_m(\gamma). \tag{3}$$

Upon solving for the coefficients A_m in Equation 3, using the orthogonality of the Legendre functions,

$$\frac{A_m}{A_o} = (2m + 1) \langle P_m(\cos \theta) \rangle \qquad (4)$$

Thus the coefficient of the m th term in the infinite series expansion for the distribution function can be determined if $\langle \cos \theta \rangle$, $\langle \cos^2 \theta \rangle$, ... $\langle \cos^m \theta \rangle$ are known. So, of course, the first coefficients are:

$$\begin{aligned} A_1/A_o &= 3\langle \cos \theta \rangle \\ A_2/A_o &= 5/2 \left[3\langle \cos^2 \theta \rangle - 1 \right] \\ A_3/A_o &= 7/2 \left[5\langle \cos^3 \theta \rangle - 3\langle \cos \theta \rangle \right] . \end{aligned} \qquad (5)$$

So the distribution function can be experimentally determined if $\langle \cos^m \theta \rangle$ can be measured. The A_m coefficients are functions of both magnetic field and magnetic history. The coefficient A_1/A_o can be determined from the M-H loop. The coefficient A_2/A_o can be determined from Equation 5 and the magnetostriction[14,15] and independently from Equation 9 and 10 of I where it is stated that the susceptibility due to domain rotation is given by:

$$\begin{aligned} \chi_p &= \frac{3}{2} \chi_o (1 - \langle \cos^2 \theta \rangle) \\ \chi_t &= \frac{3}{4} \chi_o (1 + \langle \cos^2 \theta \rangle) . \end{aligned} \qquad (6)$$

A_3/A_o can be determined from a knowledge of A_1/A_o and the use of Equations 16 of I, relating the differential magnetostrictions, namely:

$$\begin{aligned} d_p &= \frac{3}{2} d_o (\langle \cos \theta \rangle - \langle \cos^3 \theta \rangle) \\ d_t &= \frac{3}{4} d_o (\langle \cos \theta \rangle + \langle \cos^3 \theta \rangle) \end{aligned} \qquad (7)$$

where $d_o = \dfrac{3\lambda_s \chi_o}{M_s}$.

Magnetic Q. (Domain Rotation)

To estimate the magnetization dependence of the magnetic Q when the susceptibility arises from domain rotation, it is convenient to start with a single crystal ferromagnet. The domain rotation effects are assumed to obey the differential equation[16]

$$\frac{\partial \underline{M}}{\partial t} = \gamma(\underline{M} \times \underline{H}) - \frac{\alpha}{M_s} \underline{M} \times \frac{\partial \underline{M}}{\partial t} \tag{8}$$

where $\underline{M}$ is the magnetic moment, γ is the magnetomechanical ratio, M_s is the spontaneous moment, $\underline{H}$ is the applied magnetic field, and α is a dimensionless parameter proportional to the power loss. The total sample moment is assumed to be the sum of moments from all crystallites. It is thus necessary to first calculate intergranular effects, then to sum up all moments over the polycrystalline sample.

Park[8] showed that if the magnetic moment of the grains neighboring a given grain averages that of the gross material, then grain size and particle interaction is described by a single constant p. p is defined by the equation

$$\underline{H} = \underline{h} - p\underline{M} \tag{9}$$

where $\underline{H}$ is the effective differential field, $\underline{h}$ is the applied differential field, and $\underline{M}$ is the gross magnetization. p is a function of the localized packing and remains essentially independent of M. p can be regarded as the demagnetizaing factor of the grain partially canceled by the moments of its neighbors.

Upon substituting Equation 9 into Equation 8 and using the additional assumptions that a large static biasing field is oriented

in the Z-direction and sinusoidal time dependence of an additional applied field, the reversible susceptibility matrix is given by: (Equation 8 of I.)

$$\chi = \frac{1}{4} \begin{pmatrix} \left[1 + \langle\cos^2\theta\rangle\right](\chi_- + \chi_+), & 2\langle\cos\theta\rangle(\chi_- - \chi_+), & 0 \\ -2\langle\cos\theta\rangle(\chi_- - \chi_+), & \left[1 + \langle\cos^2\theta\rangle\right](\chi_- + \chi_+), & 0 \\ 0, & 0, & 2\left[1 - \langle\cos^2\theta\rangle\right](\chi_- + \chi_+) \end{pmatrix} \quad (10)$$

where $\langle\ \rangle$ represents the average value in the polycrystal and θ represents the angle between the spontaneous moment and the applied field. The susceptibilities $\chi_\pm$ are defined by the equation

$$\chi_\pm = \frac{M_x \pm iM_y}{H_x \pm iH_y}, \quad (11)$$

where M_x and H_x are the components of the differential magnetization and field in the x direction and $i = \sqrt{-1}$. The i operator represents a spatial rotation of $\pi/2$ radians. The resultant algebra from combining Equations 8,9, and 11 for the Q of the elements on the diagonal of Equation 10, yields:

$$Q^r = \frac{\omega_o}{\alpha\omega} \frac{1 - \left(\frac{\omega}{\omega_o}\right)^2 (1 - \alpha^2)}{1 + \left(\frac{\omega}{\omega_o}\right)^2 (1 + \alpha^2)} \quad (12)$$

where ω is the applied radian frequency and $\omega_o = \gamma H_t$. H_t, in turn, is the sum of the static applied and anisotropy fields, H_{ap} and H_{an}, and the effective internal field pM.

Thus:

$$H_t = H_{ap} + H_{an} + pM \quad . \quad (13)$$

In the low frequency limit:

$$Q^r = \frac{\omega_o}{\alpha\omega} \quad . \tag{14}$$

Note that Q^r is independent of field direction. The low frequency initial susceptibility is obtained by combining Equations 5 and 10 of I. The result is:

$$\chi_o = \frac{2\omega_1}{3\omega_o} \tag{15}$$

where $\omega_1 = \gamma M_s$. Combining Equations 14 and 15,

$$\chi_o Q^r = \frac{2\omega_1}{3\alpha\omega} \quad . \tag{16}$$

The product depends upon α and directly measureable quantities, and does not explicitly contain the biasing magnetic field through ω_o.

Magnetic Q. (Wall Motion)

The change in magnetic moment due to 180° wall movement is, in unit volume, given by:

$$\Delta M = \sum_k 2M_s A_k x_k \tag{17}$$

where A_k is the area of the k th wall, and x_k is the distance through which it is moved by an applied magnetic field H. The wall movement is presumed to be governed by the differential equation:

$$2\mu_o M_s H = f_k x_k + \beta \frac{dx}{dt}k + m\frac{d^2x}{dt^2}k \tag{18}$$

where f_k is the restoring constant for the k th wall, β depends upon the structure insensitive properties of the material and the parameter α of Equation 8, while m depends only upon the structure insensitive

properties of the material. μ_o is the permeability of free space.

Combining Equations 17 and 18, the wall motional reversible susceptibility under sinusoidal excitation is found to be:

$$\chi_w = 4\mu_o M_s^2 \sum_k \frac{A_k}{f_k} \left[\frac{(1 - \omega^2 \frac{m}{f_k}) - j\omega \beta/f_k}{(1 - \omega^2 \frac{m}{f_k})^2 + \omega^2 \frac{\beta^2}{f_k^2}} \right] . \qquad (19)$$

In the low frequency limit, the real susceptibility and the Q become:

$$\chi^w = 4\mu_o M_s^2 \sum_k \frac{A_k}{f_k} \qquad (20)$$

$$Q^w = \frac{1}{\omega\beta} \frac{\sum A_k/f_k}{\sum A_k/f_k^2} . \qquad (21)$$

Thus for a given material at a fixed low frequency, the Q varies only with β, A_k, and f_k.

The reversible susceptibility is given as a function of magnetization not only by the detailed mechanistic Equation 20 above, but also by Equations 2 and 18 of I. From these, if $\chi_p^w = \chi_t^w = \chi_o$ for virgin material with M = 0 and if χ_p decreases montonically with increasing M, then so must χ_t. Indeed the susceptibilities are related by the equation:

$$\chi_p^w = \left[\frac{\chi_t^w}{1 - \frac{d \ln \chi_t^w}{d \ln M}} \right] . \qquad (22)$$

If the average stiffness term f_k increases with magnetization, then so will Q. Since both A_k and f_k vary with field orientation, the parallel and transverse Q's will, in general, differ. This feature is distinctly different from domain rotation.

Initial and Remanent Susceptibility

The initial susceptibility due to domain wall motion has been approximated by Bozorth[17] for sinusoidal internal strains arising from magnetostrictive forces present when annealed material is cooled below the Curie temperature. The result is

$$\chi_o = \frac{4\mu_o M_s^2}{3\pi \lambda_s^2 E} \tag{23}$$

where λ_s is the saturation magnetostriction and E is the Young's Modulus of the material. Likewise the initial susceptibility due to domain rotation can be approximated as

$$\chi_o = \frac{2\mu_o M_s^2}{3K_1} \tag{24}$$

where μ_o is the permeability of free space and K_1 is the first order anisotropy constant. From Equations 23 and 24 it is apparent that in pure material the relative importance of the two susceptibility mechanisms depends upon the relative magnitudes of the effective anisotropy and magnetostrictive energy densities in the material.

For material with susceptibility arising by domain rotation, the relationship between the initial susceptibility and the resonant frequency should satisfy the equation:

$$f_o = \frac{2\gamma M_s}{2\pi \cdot 3\chi_o} \tag{25}$$

where γ is a constant, taken to be 2.21 x 10^5 m/amp-sec, f_o is the resonant frequency, M_s is the spontaneous moment of the material, and χ_o is the initial susceptibility.

Becker and Doring[18] discuss a model of magnetic remanence whereby, as the field is decreased from the saturation value to zero, the moments rotate to occupy the same "easy" crystallographic directions occupied in virgin material, except that all components initially anti-parallel to the saturation direction become parallel. For this model, the remanent magnetization is 0.5 M_s and the remanent rotational reversible susceptibilities equal the initial rotational susceptibility. This model is valid for hexagonal material with $K_1 > 0$. Fomenko[9] used it to interpret his permeability spectrum results. If this is also the position of maximum parallel and minimum transverse field susceptibility, then going around the M-H loop the parallel susceptibility peak occurs for M decreasing in magnitude. The remanent and initial susceptibilities will be equal.

The rotational model of gross flux change in cubic crystals would predict moments oriented in the "easy" directions nearest the field directions at remanence. For this case the remanent and rotational susceptibilities taken from the results of I are given in Table 1 for all anisotropy coefficients except K_1 equal zero. (These are the expected values from reference 1 for $\eta \longrightarrow \infty$).

Table 1
Remanent Results, M_r/M_s

	Cubic $K_1 < 0$	Cubic $K_1 > 0$	Hexagonal $K_1 < 0$	Hexagonal $K_1 > 0$
M/M_s	.500	.866	.831	.785
χ_p^r/χ_o^r	1.000	.366	.449	.500
χ_t^r/χ_o^r	1.000	1.318	1.276	1.250

An analysis of the relationships between remanent conditions and the reversible susceptibility has been carried out by Frei and Shtrikman[19] on the assumption that the reversible susceptibility is due to domain rotation. Their analysis contains the assumption that the reversible quantities are due to rotation and that the expansion of magnetization in terms of applied field must obey the rotational equations through second order in the ratio of applied to anisotropy fields, as can be seen from their Equation 10. Their resulting Equation 29 can be put in the form:

$$\frac{M_r}{M_s} = \frac{2M_s\chi_p}{(\chi_p + 2\chi_t)^2}\left[\frac{d(\chi_p + 2\chi_t)}{dM}\right] \qquad (26)$$

for comparison with experimental values.

EXPERIMENTAL

Samples Measured

Four samples were subjected to detailed measurements and are reported here. The compositions of the samples are listed in Table 2. All except the magnesium ferrite sample were fabricated at the University of Michigan.

Table 2
Composition of Ferrites Surveyed

Designation	Composition
F-1-2	$Ni_{.467}Zn_{.533}Fe_2O_4$
F-6-2	$Ni_{.168}Zn_{.533}Co_{.299}Fe_2O_4$
AA-107-4	$Fe_5Y_3O_{12}$
I-15-1	$MgFe_2O_4$

The samples with designation starting F-1 and F-6 were prepared by first ball milling the C.P. oxides weighed to the desired composition in acetone, then decanting, drying and pressing into a toroidal pill. They were then heated rapidly to 1150° C, then heated slowly to 1375° C for one-half hour, then slowly cooled to 1200° and held for two hours. The furnace was then flushed with nitrogen and deenergized. The I-15-1 core was prepared by Dr. D.L. Fresh and is from the same material reported on previously by Rado, et al,[20] as their type F core. The AA-107-4 core was prepared by firing in air at 1350° C for four hours. The mixing and pressing procedure was the same as for the type F-1 and F-6 cores.

Procedures and Techniques

All measurements were taken at ambient temperatures on toroidal samples, since this geometry avoids the complexities of demagnetizing factors. Coaxial line techniques were utilized for the spectral measurements. The complex susceptibility of the F-6 samples was measured from 1.0 to 40 mc using the radio frequency permeameter in conjunction with a Q meter. For the F-1 samples the real susceptibility from 0.1 to 40 mc and the imaginary susceptibility from 0.1

to 1.5 mc was measured using the permeameter. A fixed length coaxial line and a radio frequency bridge was used for the remaining higher loss measurements up to 50 mc. From 50 to 5000 mc, variable length coaxial cavity methods were used for complex susceptibility measurements on both types of samples.

The susceptibility and Q for the variable field measurements were taken with a Q-meter. For the transverse field measurements, the sample was placed between the pole faces of an electromagnet. The biasing field was along the axis of the toroid. Girdle windings about both outer and inner periphery of the toroid were used to determine the field and magnetization. An extra winding was placed about the toroid to furnish the biasing magnetic field when the parallel field measurements were taken.

F-6 Samples. Two different samples of F-6 material code designated F-6-1 and F-6-17 were measured for the frequency spectra. The initial spectrum of F-6-1 is shown in Figure 1. Both initial and the remanent, parallel spectra of F-6-17 are shown in Figure 2. All spectra show but a single resonant peak in the real susceptibility. The resonant frequency as determined by the peak in the imaginary susceptibility is seen to be about 130 mc for F-6-1 with a corresponding low-frequency susceptibility of 47. For F-6-17, the resonant frequency is about 75 mc with an initial low-frequency of about 82. The remanent loss for F-6-17 also peaked at 80 mc, with a low frequency susceptibility of 75. An instability of a few percent was noted in both samples between different measuring runs.

Comparing the initial and remanent curves, it is apparent that the positions of the peak in both real and imaginary susceptibilities

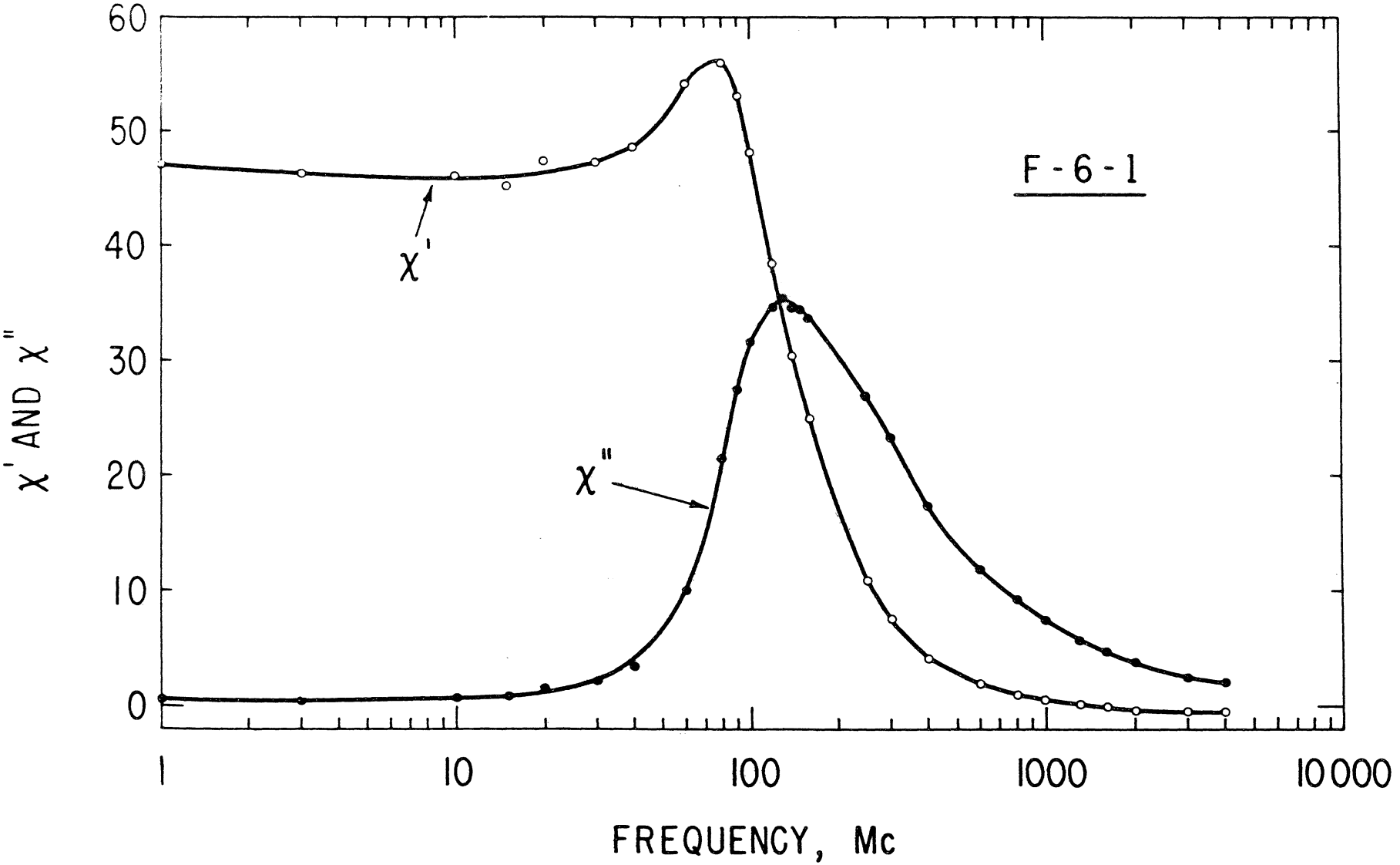

Figure 1

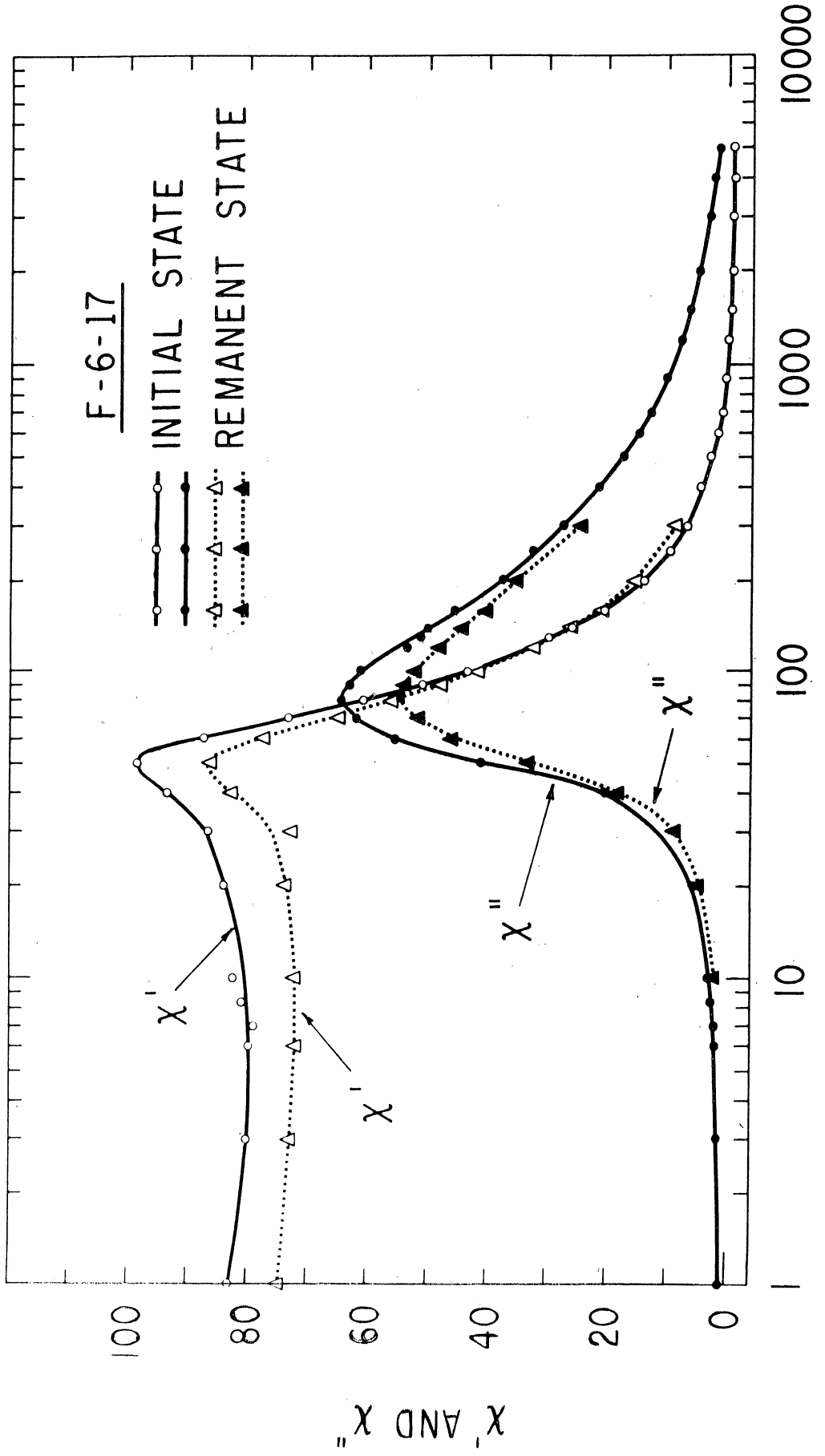
F-6-17
INITIAL STATE
REMANENT STATE
χ'
χ''
χ'
χ''
χ' AND χ''
FREQUENCY, Mc
0
20
40
60
80
100
1
10
100
1000
10000

Figure 2

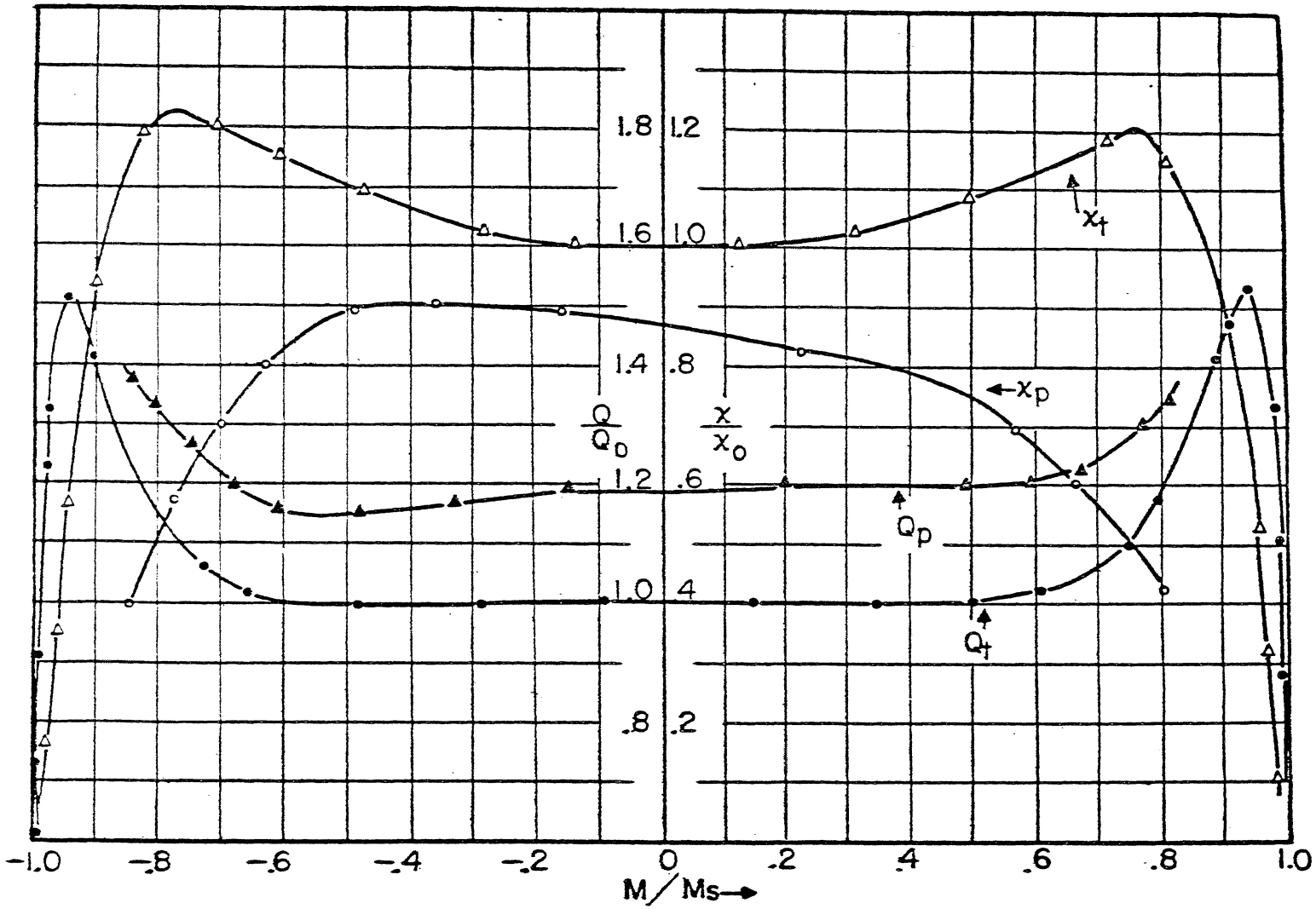

PARALLEL AND TRANSVERSE FIELD SUSCEPTIBILITIES, CORE F-6-2

Figure 3

occur at essentially the same frequency, and that the ratio of remanent to initial susceptibility is about 0.91.

The variation of the low-frequency susceptibility with magnetization is depicted in Figure 3. These data were taken on sample F-6-2. The transverse susceptibility passes through a decided minimum near M = 0. Both the measured Q's are essentially constant over a wide range of magnetization, and indeed were never observed to rise to a value equal to twice the initial value.

F-1 Samples. The spectra of the sample code designated F-1-5 was tested. Figure 4 shows the complex susceptibility for both initial and parallel remanent states. The initial spectra of F-1-6 was also measured and found to be similar in all respects to F-1-5. The resonant frequency of F-1-5 was measured as 4.5 mc as determined by the peak in the imaginary value. The low-frequency susceptibility was measured as 561. The ratio of remanent to initial value of susceptibility was 0.66. The peak in imaginary susceptibility at remanence occured at about 6 mc.

The susceptibility was measured as a function of the magnetization on specimen F-1-2, see Figure 5. For this core, the transverse susceptibility remained essentially constant over a wide range of magnetization values. The Q's pass through a minimum near M = 0. As in the case of F-6-2, the transverse susceptibility remained always larger than the parallel value. The Q's increased rapidly with increasing field to a value more than 10 times the initial value.

I-15-1. The frequency spectrum for this material has been published by Rado, Folen, and Emerson,[20] and corresponds to their "Ferrite F". They conclude that the low-frequency susceptibility is predominately

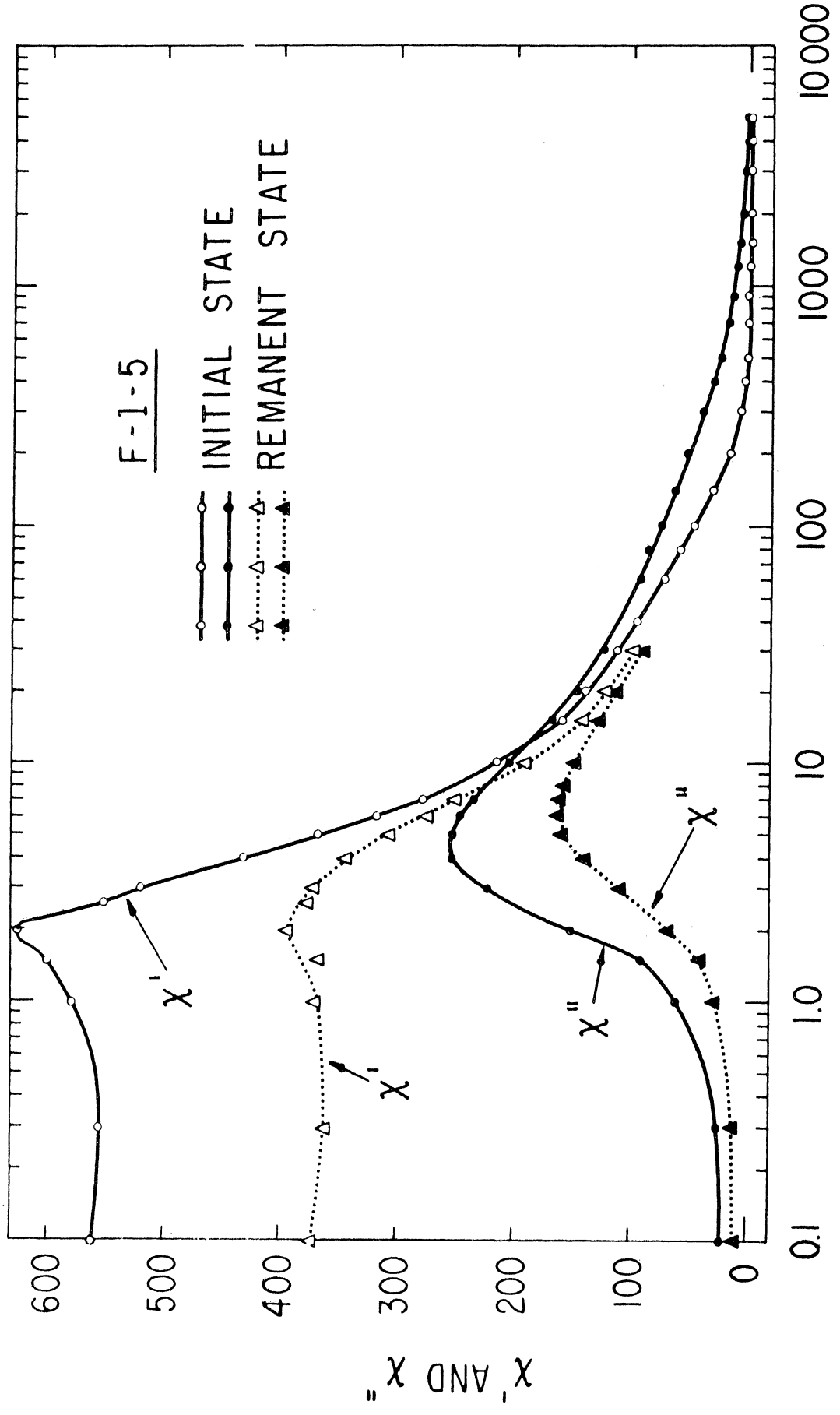
F-1-5
INITIAL STATE
REMANENT STATE
χ'
χ''
χ'
χ''
χ' AND χ''
FREQUENCY, Mc
0
100
200
300
400
500
600
0.1
1.0
10
100
1000
10000

Figure 4

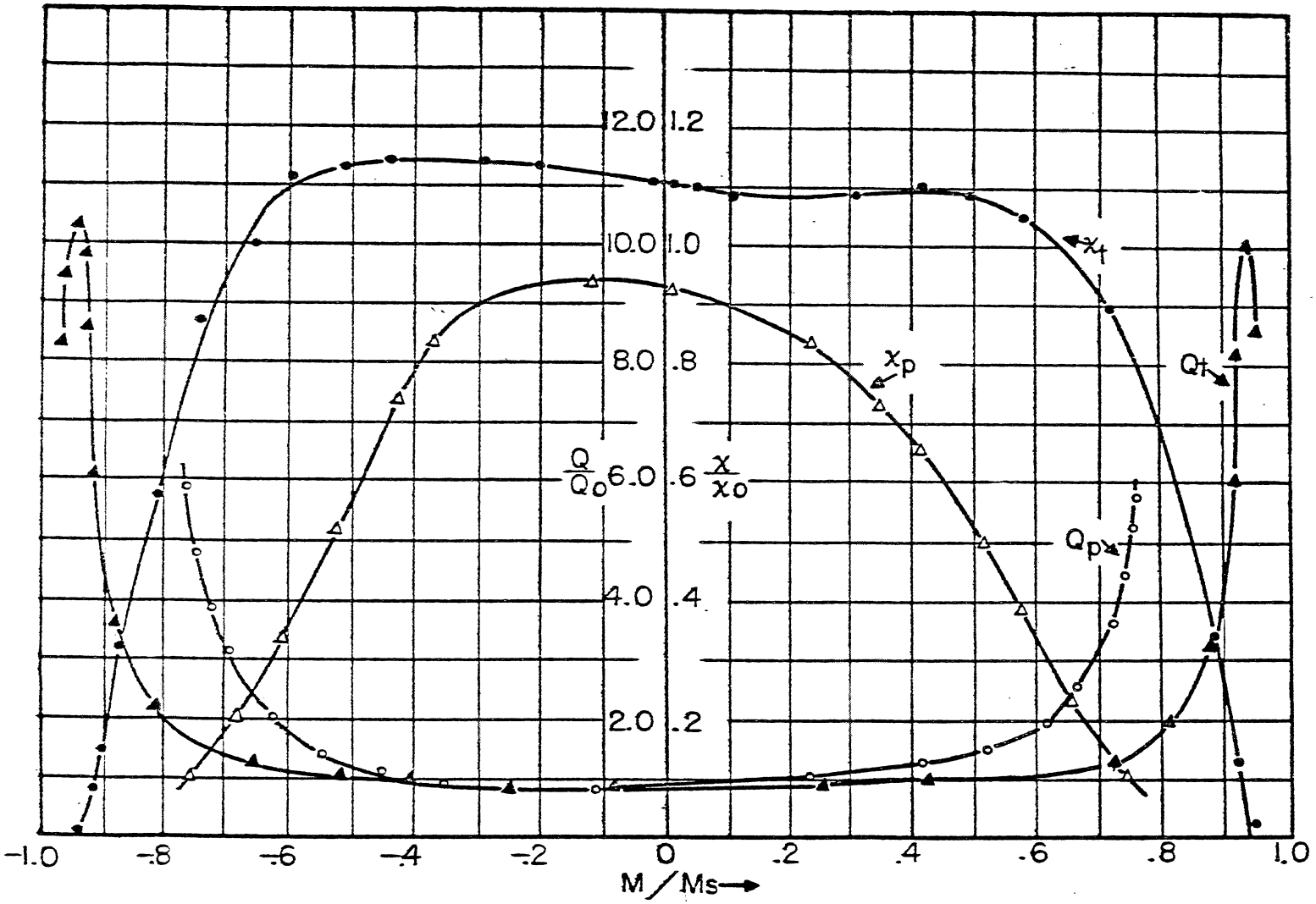

PARALLEL AND TRANSVERSE FIELD SUSCEPTIBILITIES, CORE F-1-2.

Figure 5

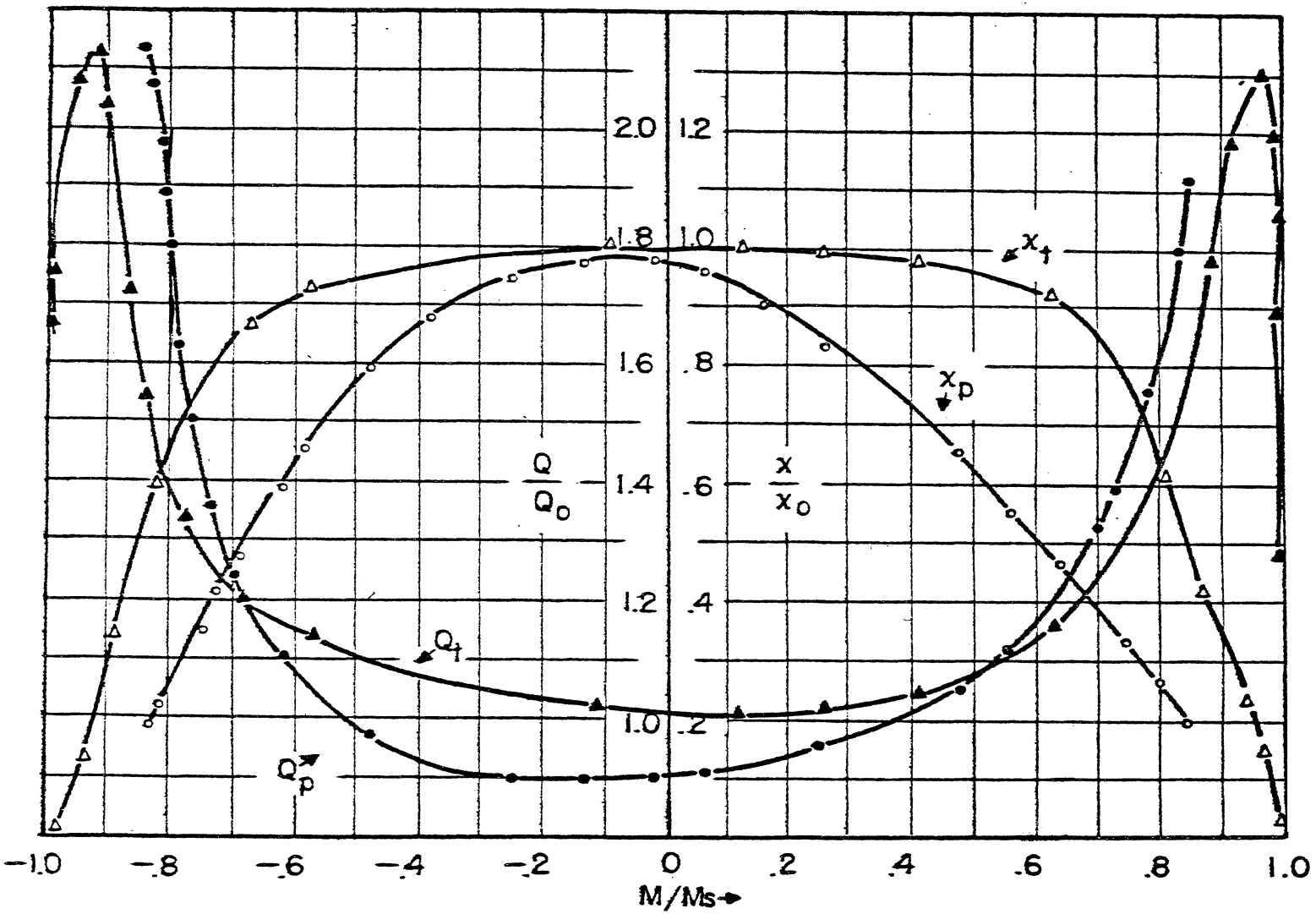

PARALLEL AND TRANSVERSE FIELD SUSCEPTIBILITIES, CORE I-15-1

Figure 6

due to the movement of domain walls. The variation of the susceptibilities with magnetization is shown in Figure 6. For this core, both the susceptibilities pass through a maximum in the vicinity of zero moment while the Q's pass through a minimum.

AA-107-4. The frequency spectra for this material has been published by two of us.[21] It was concluded on the basis of spectral information that the susceptibility was predominately due to domain wall motion. The variation of the susceptibilities with magnetization is shown in Figure 7. The transverse susceptibility does not pass through a minimum.

INTERPRETATION OF RESULTS

The values of f_o measured experimentally are listed in Table 3, along with the values calculated using Equation 25. The experimental value of f_o was determined by the frequency of the peak value of imaginary susceptibility.

Table 3
Resonant Frequency, mc.

Sample Type	Measured	Calculated	$\frac{\chi_p(M=0)}{\chi_p(H=0)}$
F-6-1	130	179	-
F-6-17	75	102	.91
F-1-2	4.5	15	.66

The expected variation of the parallel susceptibility with magnetization can be computed from the transverse susceptibility dependence. For the case of wall-motional susceptibility, Equation 22 is the proper

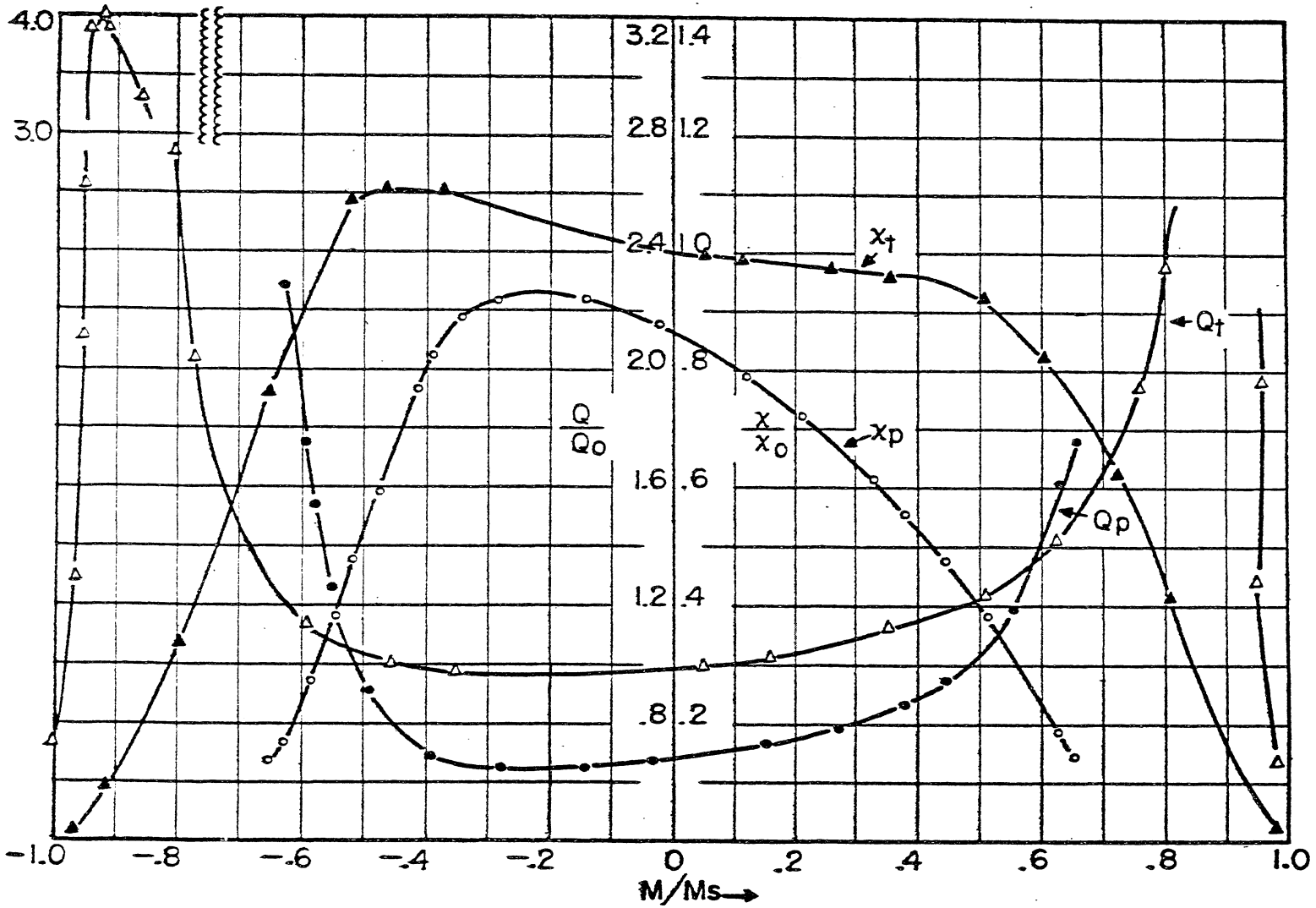

PARALLEL AND TRANSVERSE FIELD SUSCEPTIBILITIES, CORE AA-107-4

Figure 7

equation. For the case of rotational susceptibility, Equation 10 of I is the proper equation. For Equation 10 to be useful, however, the variation of χ_o with applied field must be known. From Equation 15 and the definition of ω_o, it follows that in the absence of a detailed knowledge of the effective anisotropy field, which is always the case for polycrystalline material, χ_o is known only so long as the biasing field is small compared with the anisotropy field.

The magnetic parameters of the four cores are listed in Table 4.

Table 4
Magnetic Parameters of Four Ferrimagnetic Cores (320 kc)

	Parallel						Transverse			
Core	χ_o**	Q_o	χ_{po}	Q_{po}	χ_{pr}	Q_{pr}	χ_{to}	Q_{to}	χ_{tr}	Q_{tr}
F-6-2	-	-	46.5	72.4	39.6	71.7	52.8	60.8	62.0	61.4
F-1-2*	410	15.2	388	13.2	135	28.1	450	13.5	448	16.7
I-15-1	-	-	54.2	38.1	33.3	53.9	54.2	39.5	43.6	49.8
AA-107-4	36.4	10.9	31.1	7.4	30.0	8.2	36.6	10.4	40.0	9.7

*Values at 500 kc.

**The subscript "o" indicates measurements in the virgin state, "p" indicates parallel and "t" transverse measurements. "po" and "to" represent measurements around the M-H loop at the position M=0 in parallel and transverse fields. "pr" and "tr" represent similar measurements at the remanent position.

Plots of χ_p computed from χ_t for each of the four samples measured are shown in Figures 8 through 11, and compared with the experimentally measured curves. It is apparent that the rotational curve fits F-6-2 well and that the wall-motional curve fits I-15-1 well. The fit is not good for either of the other specimens, but nonetheless the

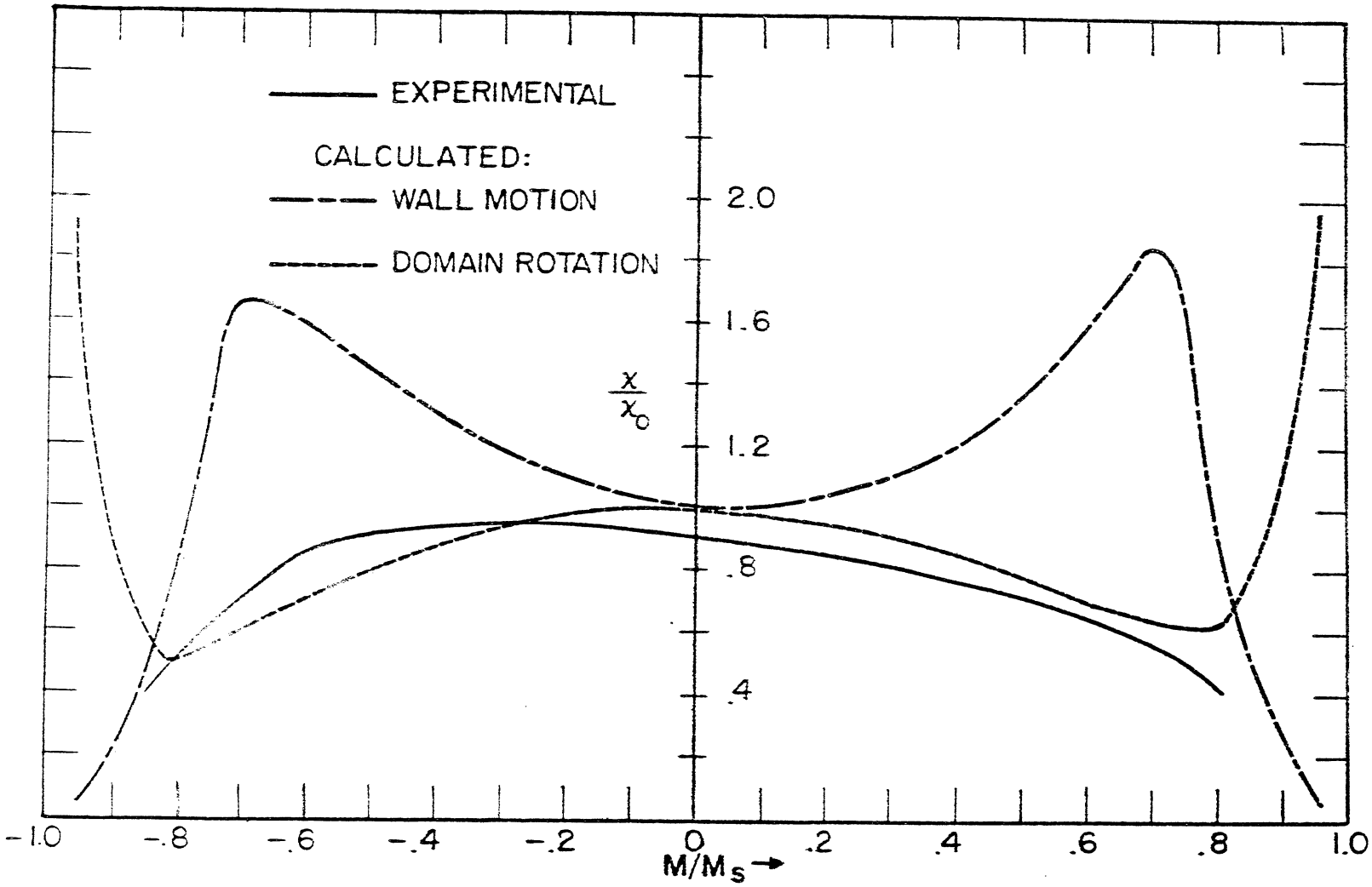

PARALLEL REVERSIBLE SUSCEPTIBILITIES, CORE F-6-2

Figure 8

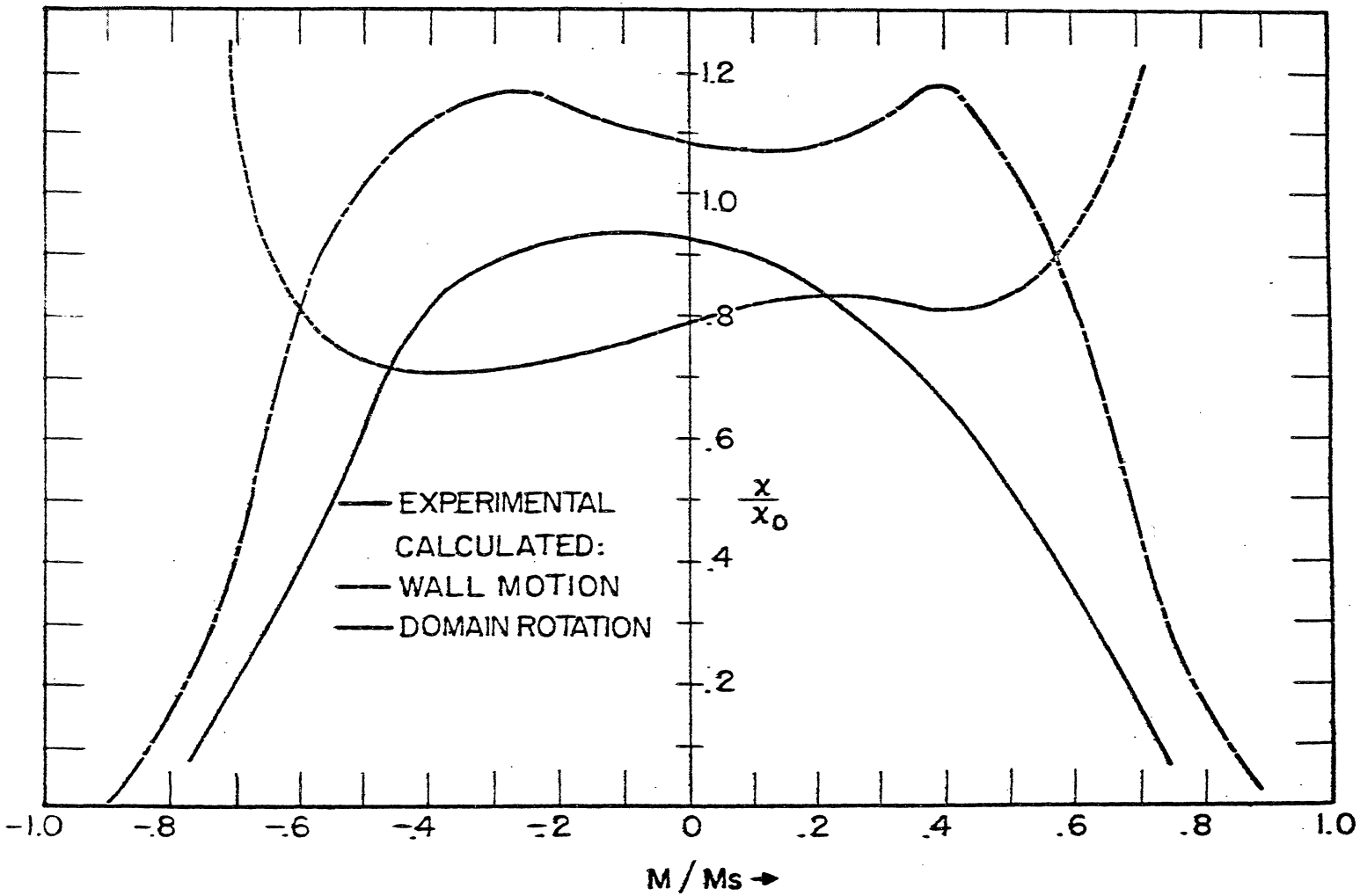

PARALLEL REVERSIBLE SUSCEPTIBILITIES, CORE F-1-2

Figure 9

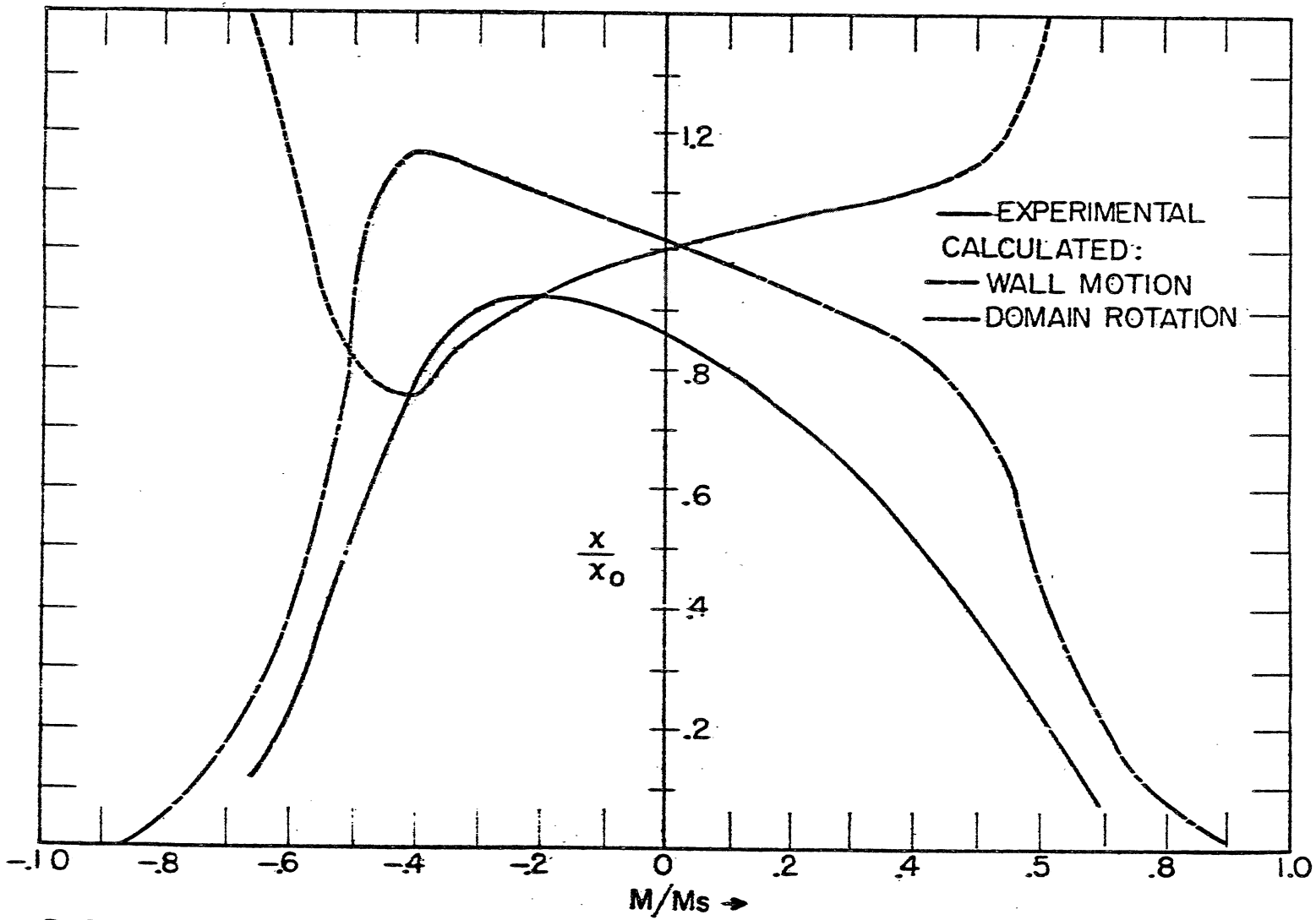

PARALLEL REVERSIBLE SUSCEPTIBILITIES, CORE AA-107-4

Figure 10

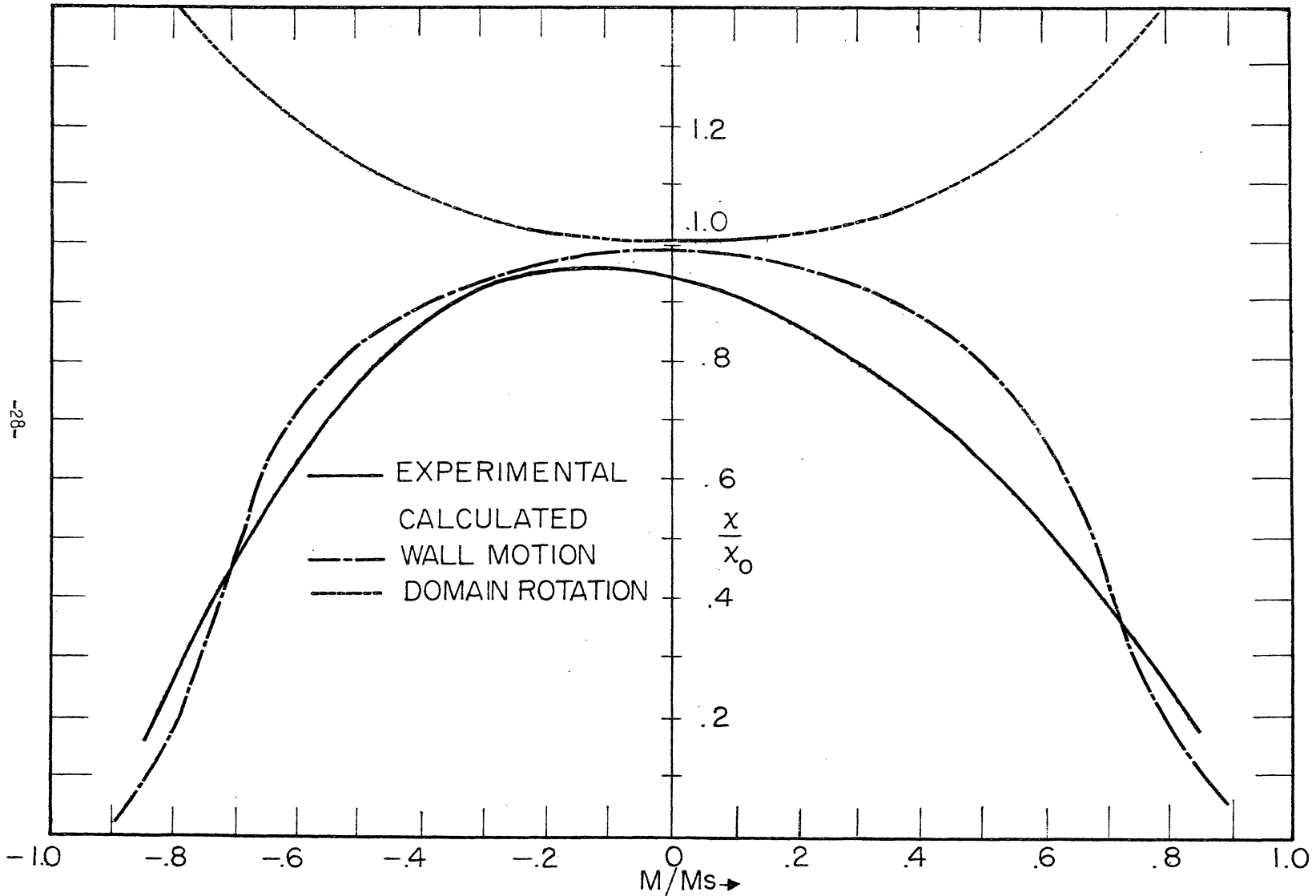

PARALLEL REVERSIBLE SUSCEPTIBILITIES, CORE I-15-1

Figure 11

wall-motional curve fits AA-107 closer than the rotational curve. The conclusion that cores F-6-2 and I-15-1 have susceptibility arising predominately from rotation and wall motion respectively is substantiated by the spectral interpretation of Figures 1 and 2 and by Rado et al.[20]

The curve calculated for χ_p for rotation is valid so long as the anisotropy field remains much larger than the applied baising field. F-6-2 contains cobalt, and therefore will have a large anisotropy field. Core F-1-2 is a mixed nickel-zinc ferrite with a corresponding small anisotropy. Thus the lack of agreement with rotational curves is not significant. For the F-1-2 core, there was a slight but real minimum in the χ_t in the vicinity of zero moment. This feature is not consistent with wall motion and the accompanying χ_p behavior. Therefore it is concluded that domain rotation must be present. No such behavior was found in AA-107. In the spectral data, two peaks in the imaginary susceptibility were observed for AA-107, and only one for F-1-2. There must, therefore, be two important mechanisms for the AA-107. These mechanisms are assumed to be rotation and wall motion. For F-1-2, one can only say that domain rotational effects enter. If wall motional effects are present, the resonant frequency must occur at the same point as the rotational effect. The essential difference between F-1 and F-6 lies in the value of anisotropy. Since rotational effects have been shown to exist in the high anisotropy material, it is expected that they should also exist in the low anisotropy material.

Material F-6-2 apparently fits the conditions imposed in this paper for the static conditions, namely oriented along easy crystallographic directions, and the susceptibility obeys the rotational equations. This material would not satisfy the conditions of

Frei and Shtrikman. Table 5 compares the values of remanent moment calculated from Equation 26 with experimentally measured values.

Table 5

Specimen	Measured M_r/M_s	Calculated M_r/M_s	H_c	M_s x 10^{-5}	M_r x 10^{-5}
AA-107-4	.389	.259	160	1.06	0.41
F-6-2	.660	.041	127	3.58	2.37
F-1-2	.610	.330	100	3.67	2.24
I-15-1	.730	.675	175	1.35	0.98

The agreement is not good, and indeed the best agreement is with the material whose susceptibility arises from wall motion.

Upon eliminating χ_o from Equation 6 the average value of $\langle \cos^2 \theta \rangle$ is found to be:

$$\langle \cos^2 \theta \rangle = \left(\frac{2\chi_t - \chi_p}{2\chi_t + \chi_p} \right) . \qquad (27)$$

Solving for $\langle \cos^3 \theta \rangle$ from Equations 7,

$$\langle \cos^3 \theta \rangle = \left(\frac{2d_t - d_p}{2d_t + dp} \right) \langle \cos \theta \rangle . \qquad (28)$$

Note that $\langle \cos^2 \theta \rangle$ should vary from 1/3 in the demagnetized state to unity when the material is saturated. A similar wall-motional equation yields:

$$\frac{2\chi_t - \chi_p}{2\chi_t + \chi_p} = \frac{1 - 2\left(\frac{d\ln \chi_t}{d\ln M}\right)}{3 - 2\left(\frac{d\ln \chi_t}{d\ln M}\right)} \qquad (29)$$

If the values of χ_t and M are calculated assuming a Boltzman distribution of moments, then $\chi_t = AM_sL(\eta)/\eta$ and $M = M_sL(\eta)$ where A is a constant for the material, $L(\eta)$ represents the Langevin function of η, and $\eta = AH_t$ where H_t is the totalized biasing field, including history, anisotropy, and applied field. Substituting these values into Equation 29 yields a function which goes from 1/3 for M = 0 to unity for saturation.

Plots of $\frac{2\chi_t - \chi_p}{2\chi_t + \chi_p}$ as a function of $\langle \cos \theta \rangle$ are shown in Figures 12 and 13. In Figure 12, the theoretical curve is the value of $\langle \cos^2 \theta \rangle$ calculated for domain rotation. In Figure 13, the theoretical curve is based upon domain-wall motion. Both curves are based upon Boltzman distribution of moments. The rotational curve attributed to domain rotation can be interpreted in terms of variation from the most probable condition. For F-6-2, as the moment is decreased, moments parallel and antiparallel are initially in excess of the most probable condition. However, as M is further decreased towards zero, the parallel-antiparallel components increase to larger than the most probable value. This can be considered the reason for the transverse susceptibility at zero moments being larger than the initial susceptibility, and the corresponding parallel susceptibility at zero moment being smaller than either. Sample F-1-2, if the susceptibility is assumed entirely rotation, maintains at all times a predominate parallel-antiparallel moment configuration. The value of A_2 from Equation 5 as a function of magnetic moment can be read directly from Figure 12 for sample F-6-2.

More detailed determinations and analyses of the distribution functions on other materials must await simultaneous parallel and transverse susceptibility and differential magnetostriction measurements.

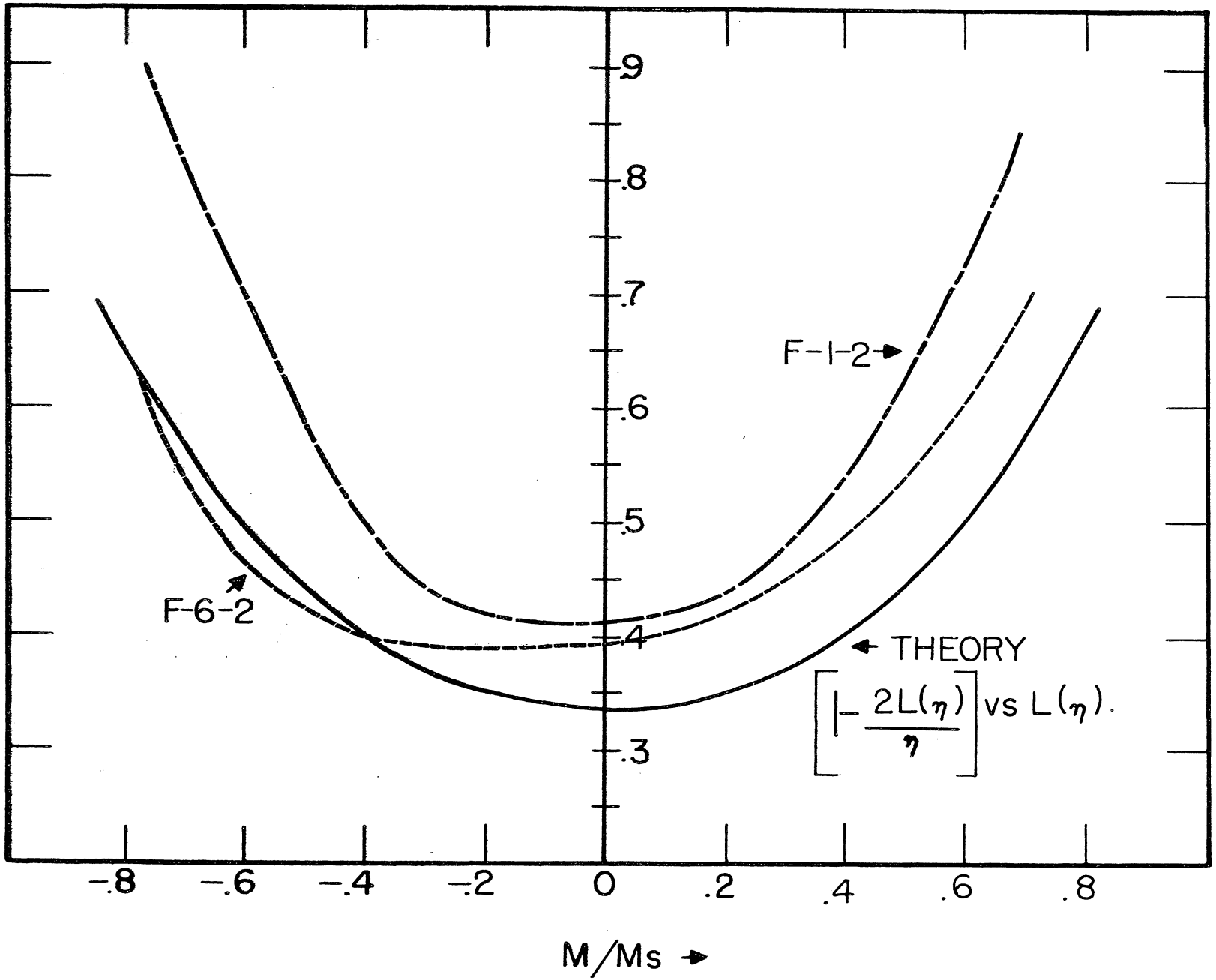

VARIATION OF $\langle \cos^2 \theta \rangle$ WITH $\langle \cos \theta \rangle$

Figure 12

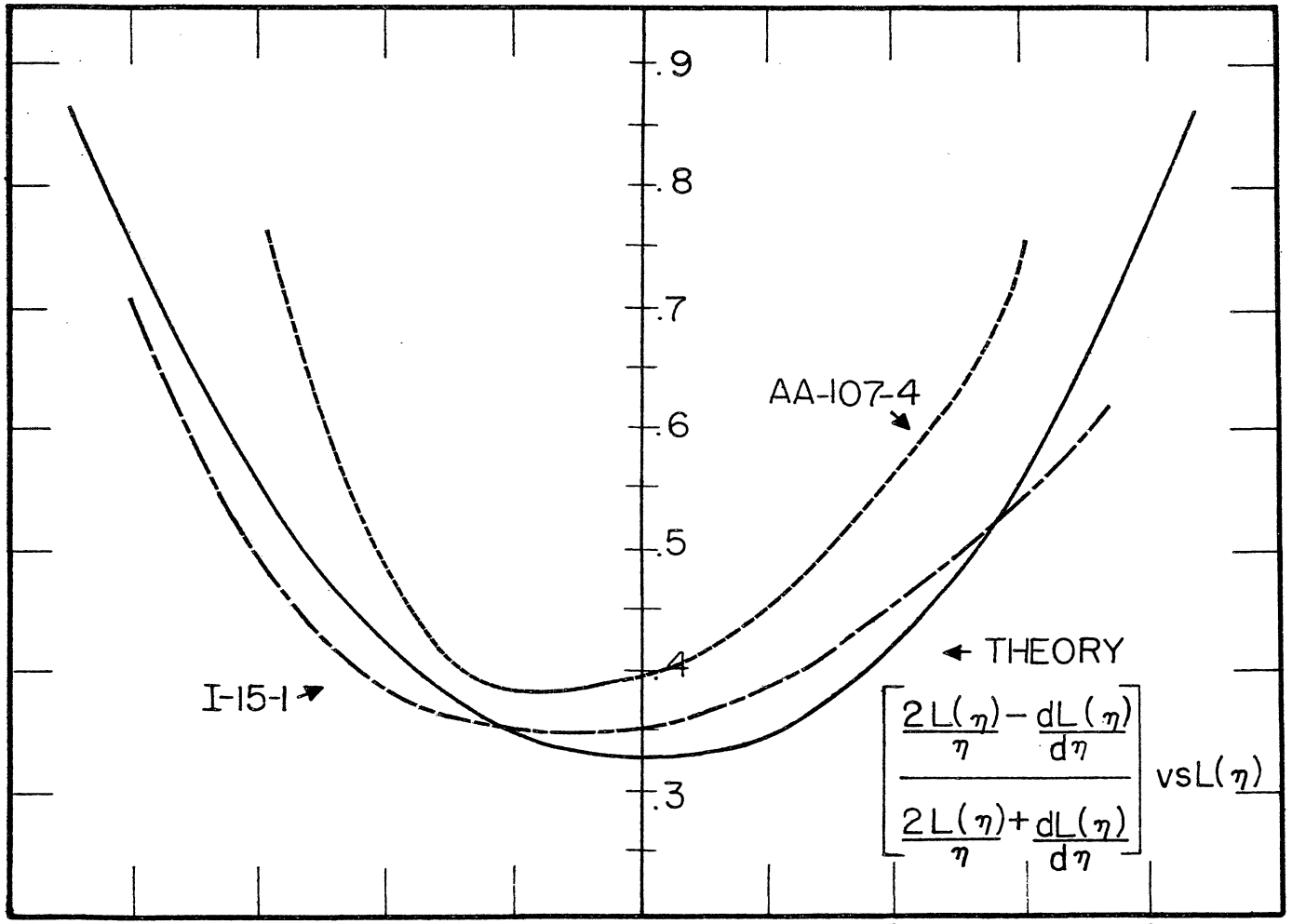

$\left[\frac{2x_t - x_p}{2x_t + x_p}\right]$ VERSUS M/Ms

Figure 13

CONCLUSIONS

The magnetic properties of a ferromagnetic system can be described in terms of a distribution of magnetic moments about the unit sphere. This function cannot be calculated in detail for macroscopic systems. However, assuming idealized models of magnetic behavior such as magnetization by domain-wall motion or magnetization by domain rotation, some reversible properties of ferromagnets can be compared without detailed knowledge of the distribution function. If a detailed distribution function is assumed, then, of course, the magnetic properties can be calculated in detail.

The inverse of this calculation can also be made. The procedure consists of firstly expanding the distribution function in an infinite series of Legendre polynomials. Due to the orthogonality properties of these functions, the coefficients of each term in the infinite series can be evaluated if the weighted average value of the proper power of $\langle \cos \theta \rangle$ over the sample is known. $\langle \cos \theta \rangle$ itself is, of course, proportional to the magnetic moment of the sample. Under certain conditions $\langle \cos^2 \theta \rangle$ is proportional to the static magnetostriction. It can also be found from a knowledge of the two reversible susceptibilities if domain rotation is the source of the susceptibility. Further, under the same susceptibility conditions, the differential magnetostriction can be utilized to find $\langle \cos^3 \theta \rangle$ and one additional coefficient in the expansion.

The combination of frequency spectra and magnetization dependence of the susceptibilities on the same types are utilized to examine the source of the susceptibility. In agreement with other investigators,

it is found that the major susceptibility source depends upon the type of ferrite, as well as the method of preparation. The nickel zinc cobalt ferrite F-6-2 shows distinctive domain rotational effects. Sample I-15-1 shows wall-motional effect.

The authors wish to acknowledge the invaluable assistance of Messrs. R.M. Olson, A.H. Voelker, and Mrs. P.A. Marchello.

BIBLIOGRAPHY

1. Grimes, D.M., "Reversible Properties of Polycrystalline Ferromagnets: I. Theory of the Expected Variation of the Reversible Properties with Magnetization," J. Phys. Chem. Solids 3, 141-152 (1957).

2. Goodenough, J.B., "A Theory of Domain Creation and Coercive Force in Polycrystalline Ferromagnetics," Phys. Rev. 95, 917-932 (1954).

3. Brown, W.F., Jr., "Criterion for uniform Micromagnetization," Phys. Rev. 105, 1479-1482 (1957).

4. Frei, E.H., Shtrikman, S., and Treves, D., "Critical Size and Nucleation Field of Ideal Ferromagnetic Particles," Phys. Rev. 106, 446-455 (1957).

5. Snoek, J.L., "Dispersion and Absorption in Magnetic Ferrites at Frequencies above One Mc/s," Physica 14, 207-218 (1948).

6. Wijn, H.P.J., Gevers, M., and Van der Burgt, C.M., "Note on the High Frequency Dispersion in Nickel Zinc Ferrites," Rev. Mod. Phys. 25, 91-92 (1953).

7. Brown, F. and Gravel, C.L., "Direct Observation of Domain Rotation in Ferrites," Phys. Rev. 98, 442-448 (1955).

8. Park, D., "Magnetic Rotation Phenomena in a Polycrystalline Ferrite," Phys. Rev. 97, 60-66 (1955).

9. Fomenko, L.A., "An Investigation of Magnetic Spectra of Solid Solutions of Some NiZn Ferrites in the Radio-Frequency Range," Soviet Physics JETP 3, 19-28 (1956).

10. Harrison, S.E., Kriessman, C.J., Pollack, S.R., "Magnetic Spectra of Manganese Ferrites," Phys. Rev. 110, 844-849 (1958).

11. Rado, G.T., Wright, R.W., Emerson, W.H., "Ferromagnetism at Very High Frequencies. III. Two Mechanisms of Dispersion in a Ferrite," Phys. Rev. 80, 273-280 (1950).

12. Epstein, D.J., "Domain Wall Relaxation in Ferrites," Boston Conference Proceedings, 493-503, T-91, AIEE, February, 1957.

13. Birks, J.B., "Magnetic Spectra," Proc. IEE, Part B Suppl. No. 5, 179-188 (1956).

14. Brown, W.F., Jr., "Domain Theory of Ferromagnets Under Stress, Part II. Magnetostriction of Polycrystalline Material," Phys. Rev. 53, 482-491 (1938).

15. Lee, E.W., "Magnetostriction Curves of Polycrystalline Ferromagnetics," Proc. Phys. Soc. Part 2, 72, 249-258 (1958).

16. Gilbert, T.L.,"The Phenomenological Theory of Ferromagnetism," Armour Research Foundation, 1 May, 1956.

17. Bozorth, R.M., Ferromagnetism, D. Van Nostrand, New York (1951), p. 822.

18. Becker, R. and Doring, Ferromagnetismus, Edward Bros., Ann Arbor, 1943.

19. Frei, E.H., and Shtrikman, S., "The Remanent State in Ferrites According to the Rotation Model," Boston Conference Proceedings, p. 504-511, T-91, AIEE, February, 1957.

20. Rado, G.T., Folen, V.J., and Emerson, W.H., "Effect of Magnetocrystalline Anisotropy of the Magnetic Spectra of Mg-Fe Ferrites," Proc. IEE, Part B, Suppl. No. 5, 198-205, (1956).

21. Harrington, R.D. and Rasmussen, A.L., "Initial and Remanent Permeability Spectra of Yttrium Iron Garnet," Proc. IRE 47, 98 (1959).

DISTRIBUTION LIST

ADDRESS	COPIES
Commander Hq., AF Office of Scientific Research, ARDC Attn: SRQB Washington 25, D.C.	5
Commander Wright Air Development Center Attn: WCRRH Attn: WCRRL Attn: WCRTL Attn: WCRTM-1 Wright-Patterson Air Force Base, Ohio	4
Commander Air Force Cambridge Research Center Attn: Technical Library Attn: CRRF L.G. Hanscom Field Bedford, Massachusetts	2
Commander Rome Air Development Center Attn: Technical Library Griffiss Air Force Base Rome, New York	1
Director, Office for Advanced Studies Air Force Office of Scientific Research P.O. Box 2035 Pasadena 2, California	1
Commander European Office, ARDC c/o American Embassy Brussels, Belgium (Inner Envelope--No postage)	1
Superintendent Diplomatic Pouch Rooms Department of State Washington 25, D.C. (Outer Envelope--bearing sufficient postage for delivery to Washington)	
Armed Services Technical Information Agency Arlington Hall Station Arlington 12, Virginia	10
Director of Research and Development Hq., USAF Attn: AFDRD-RE-3 Washington 25, D.C.	1
Department of the Navy Office of Naval Research Attn: Code 423 Attn: Code 421 Washington 25, D.C.	2
Officer in Charge Office of Naval Research Navy No. 100 Fleet Post Office New York, New York	1
Commanding Officer Naval Radiological Defense Laboratory San Francisco Naval Shipyard San Francisco 24, California	1
Director, Research and development Division General Staff Department of the Army Washington 25, D.C.	1

ADDRESS	COPIES
Division of Research U.S. Atomic Energy Commission Division Office Washington 25, D.C.	1
U.S. Atomic Energy Commission Library Branch Technical Information Division, ORE P.O. Box E Oak Ridge, Tennessee	1
Oak Ridge National Laboratory Attn: Central Files Post Office Box P Oak Ridge, Tennessee	1
Brookhaven National Laboratory Attn: Research Library Upton, Long Island, New York	1
Argonne National Laboratory Attn: Librarian P.O. Box 299 Lemont, Illinois	1
Ames Laboratory Iowa State College P.O. Box 14A, Station A	1
Knolls Atomic Power Laboratory Attn: Document Librarian P.O. Box 1072 Schenectady, New York	1
National Bureau of Standards Library Room 203, Northwest Building Washington 25, D.C.	1
National Science Foundation 1901 Constitution Avenue, N.W. Washington 25, D.C.	1
Director, Office of Ordnance Research Box CM, Duke Station Durham, North Carolina	1

ADDRESS	COPIES
Office of Technical Services Department of Commerce Washington 25, D.C.	1
Commander Western Development Division ARDC Attn: WDSIT P.O. Box 262 Inglewood, California	1
Document Custodian Los Alamos Scientific Laboratory P.O. Box 1663 Los Alamos, New Mexico	1
Arnold Engineering Development Center Attn: Technical Library P.O. Box 162 Tullahoma, Tennessee	1
Commanding Officer Ordnance Materials Research Office Watertown Arsenal Watertown 72, Massachusetts	1
Commanding Officer Watertown Arsenal Watertown 72, Massachusetts Attn: Watertown Arsenal Labs. Technical Reports Section	1
National Advisory Committee for Aeronautics 1512 H. Street, N.W. Washington 25, D.C.	1
Commander Air Technical Intelligence Center Attn: Deputy for Documentation Wright-Patterson Air Force Base Ohio	1

ADDRESS	COPIES
Commander Hq., AF Office of Scientific Research Attn: SREC Attn: Technical Library Washington 25, D.C.	2
Commandant AF Institute of Technology Attn: Technical Library MCLI Wright-Patterson Air Force Base Ohio	1
Commander Wright Air Development Center Attn: WCLTY-3 Mr. Robert Besamson Wright-Patterson Air Force Base Ohio	1
Prof. A.H. Morrish Department of Electrical Engineering University Of Minnesota Minneapolis, Minnesota	1
Dr. W.F. Brown, Jr. Department of Electrical Engineering University of Minnesota Minneapolis, Minnesota	1
Dr. R.J. Prosen Honeywell Research Center Hopkins, Minnesota	1
L.E. Blazier, Research Library A.C. Sparkplug Division, G.M.C. Flint 2, Michigan	2
Dr. L. Reiffel, Manager Physics Research Armour Research Foundation 3440 South State Street Chicago 16, Illinois	1
Dr. Nat Schwartz, Bldg. 3 Electronics Park General Electric Co. Syracuse, N.Y.	1

ADDRESS	COPIES
Dr. G.T. Rado Naval Research Laboratory Washington 25, D.C.	1
Mr. John L. Dalke, Div. 84.30 National Bureau of Standards Boulder, Colorado	1
Dr. D.M. Grimes Department of Electrical Engineering University of Michigan Ann Arbor, Michigan	8
Dr. H. Katz, Bldg. 3 Electronics Park General Electric Co. Syracuse, New York	1
Central File University of Michigan Research Institute 132A Cooley Bldg. Ann Arbor, Michigan	1
Mr. Peter H. Haas Mine Fuze Division Diamond Ordnance Fuze Labs. Washington 25, D.C.	1
Dr. R.M. Bozorth Bell Telephone Laboratories Murray Hill, New Jersey	1
Mr. John A. Osborn, Mgr. Magnetic Materials Development Section Westinghouse Electric Corp. 501 Highland Avenue East Pittsburgh, Pa.	1
Mr. Robert Harrington Div. 84.30 National Bureau of Standards Boulder, Colorado	1
Dr. John B. Goodenough Lincoln Laboratory, MIT Cambridge, Massachusetts	1
Frank R. Arams Airborne Instruments Laboratory Mineola, Long Island, N.Y.	1